

Forced Vibrations of Functionally Graded Plates in the Three-Dimensional Setting

Isaac Elishakoff*

Florida Atlantic University, Boca Raton, Florida 33431-0991

and

Cristina Gentilini[†] and Erasmo Viola[‡]

University of Bologna, 40136 Bologna, Italy

The approach by Siu and Bert and by Leissa that was originally developed for isotropic plates is extended to the problem of forced damped vibrations of functionally graded simply supported rectangular plates in the three-dimensional setting. Contrary to classical normal mode analysis, in this study the forced-vibration response is determined without prior solving the free-vibration problem. The solution is obtained by the Rayleigh–Ritz method, extended to include the damping term and the work done by the external excitation. Numerical results are presented for a two-phase graded material with a power law variation of the volume fraction of the constituents through the thickness. As a byproduct, the natural frequencies and the static solution are also determined. The dynamic response as well as exact natural frequencies of homogeneous plate are used to assess the accuracy of the present formulation. A parametric study with respect to varying volume fraction of the constituents and thickness ratio is conducted. The analysis is applied to predict the dynamic response of a functionally graded plate subjected to a harmonically exciting force on its top surface.

Nomenclature

a, b, h	= plate dimensions
c	= equivalent viscous damping of the functionally graded material (FGM) plate
c_{c1}	= critical damping
c_1, c_2	= damping coefficients of the ceramic and metal
\mathcal{D}	= dissipation functional
E	= modulus of elasticity of the FGM plate
E_1, E_2	= moduli of elasticity of the ceramic and metal
F_u, F_v, F_w	= boundary functions
N	= power law exponent
P	= arbitrary material property
$P_s(\chi)$	= sth Chebyshev polynomial
P_1, P_2	= arbitrary material properties of the ceramic and metal
q	= harmonically exciting force
q_0	= transverse uniform load
\mathcal{T}	= kinetic energy
U, V, W	= displacement amplitudes in x, y, z directions
\mathcal{V}	= strain energy
V_1, V_2	= volume fractions of the ceramic and metal
\mathcal{W}	= work done by external forces
γ	= frequency ratio
δ_1	= damping ratio
ν	= Poisson's ratio of the FGM plate
ν_1, ν_2	= Poisson's ratios of the ceramic and metal
ρ	= mass density of the FGM plate
ρ_1, ρ_2	= mass densities of the ceramic and metal

ω	= forcing frequency
$\varpi(\chi)$	= weight function of Chebyshev polynomials

Subscripts

1, 2	= ceramic, metallic constituents
------	----------------------------------

Introduction

THE demand for improved structural efficiency in space structures has resulted in development of a new class of materials, called functionally graded materials^{1–3} (FGMs). The continuous change in the material properties, for example, in the modulus of elasticity, from one surface of the material to the other surface, distinguishes FGMs from conventional composite materials. A common structural element for such applications is the simply supported rectangular plate, for which several recent studies on statics, buckling, and free vibrations have been performed. The nonlinear dynamic analysis of plates made of functionally graded materials, under thermal and mechanical loading, was studied by Praveen and Reddy⁴ using a shear deformable finite element developed within the von Kármán plate theory. Reddy's higher-order plate theory has been employed by Cheng and Batra⁵ to seek the exact correspondence between the eigenvalues of membranes and those of FGM plates subjected to uniform in-plane loads. Reddy⁶ developed a finite element model based on the third-order shear deformation plate theory for the nonlinear static and dynamic analyses of through-thickness functionally graded plates. Ng et al.⁷ studied the dynamic stability of FGM simply supported rectangular plates under static and periodic in-plane loadings. Yang and Shen⁸ analyzed the free and forced vibration for initially stressed functionally graded rectangular plates in thermal environment. Vibration characteristics of functionally graded shells were studied by Pradhan et al.⁹ and Yang and Shen¹⁰ using Love's theory and Reddy's higher-order shear deformation shell theory, respectively. A semi-analytical method based on differential quadrature technique was proposed by Yang et al.¹¹ and by Kitipornchai et al.¹² to solve the problem of large-amplitude vibrations of FGM laminated plates with two clamped edges and with geometric imperfections, respectively. Recently, Vel and Batra¹³ presented a three-dimensional solution for free and forced vibrations of simply supported functionally graded plates by employing the power series method, without considering damping.

It must be stressed that it is important to be able to predict the dynamic response including the effects of damping. To the best of our

Received 31 August 2004; revision received 31 March 2005; accepted for publication 4 April 2005. Copyright © 2005 by the authors. Published by the American Institute of Aeronautics and Astronautics, Inc., with permission. Copies of this paper may be made for personal or internal use, on condition that the copier pay the \$10.00 per-copy fee to the Copyright Clearance Center, Inc., 222 Rosewood Drive, Danvers, MA 01923; include the code 0001-1452/05 \$10.00 in correspondence with the CCC.

*J. M. Rubin Foundation Distinguished Professor, Department of Mechanical Engineering, 777 Glades Road; elishako@fau.edu.

[†]Ph.D. Student, Dipartimento di Ingegneria delle Strutture, dei Trasporti, delle Acque, del Rilevamento, del Territorio (DISTART), viale Risorgimento 2; cristina.gentilini@mail.ing.unibo.it.

[‡]Professor, Dipartimento di Ingegneria delle Strutture, dei Trasporti, delle Acque, del Rilevamento, del Territorio (DISTART), viale Risorgimento 2; erasmo.viola@mail.ing.unibo.it.

knowledge, no detailed solutions have been published on vibrations of functionally graded simply supported rectangular plates, which include damping.

The present analysis represents an extension of the works by Siu and Bert,¹⁴ Leissa,^{15–17} and Elishakoff et al.¹⁸ to simply supported FGM plates in the three-dimensional setting. The classical method for analyzing the forced vibrations of structural elements is to express the displacements as superposition of the free-vibration modes. This is only possible for those relatively few problems where the exact eigenfunction solutions exist. According to Leissa, “mode shapes usually are not known with sufficient accuracy to give meaningful results for stresses.” On the other hand, the Ritz method is widely used to obtain approximate solutions for free undamped vibration problems. The present paper demonstrates how the same method can be generalized to analyze forced vibrations of a rectangular functionally graded plate with damping. This is done directly without requiring the free-vibration eigenfunctions. Appropriate functionals representing the forcing and damping terms are discussed.

In this study, a ceramic-metal graded plate with a power-law variation of the volume fraction of the constituents in the thickness direction is considered. Chebyshev polynomials multiplied by appropriate boundary functions, such that they satisfy the boundary conditions, are assumed as admissible functions to represent the displacement amplitudes. Numerical results are obtained for different values of the power-law exponent and thickness-side ratio.

Statement of the Problem

A rectangular plate made of a two-phase functionally graded material is considered. The middle plane of the plate is taken as reference plane, and the origin of the Cartesian coordinate system ($O; x, y, z$) is the geometric center of this plane. For simplicity, the nondimensional coordinate system ($O; \xi, \eta, \zeta$) is introduced:

$$\xi = 2x/a, \quad \eta = 2y/b, \quad \zeta = 2z/h \quad (1)$$

where a , b , and h are the plate length, the plate width, and the uniform thickness, respectively.

It is assumed that the FGM is made of a mixture of a ceramic (material 1) and a metallic (material 2) component. The arbitrary material property, denoted as P , of the functionally graded plate is assumed to vary smoothly through the thickness of the plate, as a function of the volume fractions and properties of the constituent materials. This property can be expressed as a linear combination

$$P(\zeta) = P_1 V_1 + P_2 V_2 \quad (2)$$

where P_1 , V_1 and P_2 , V_2 are the corresponding material properties and volume fractions of the ceramic and metal, respectively. The volume fractions of all of the constituent materials should add up to unity:

$$V_1 + V_2 = 1 \quad (3)$$

For a plate with the reference surface at its middle surface, the volume fraction can be written as

$$V_1 = \left(\zeta/2 + \frac{1}{2}\right)^N, \quad V_2 = 1 - \left(\zeta/2 + \frac{1}{2}\right)^N \quad (4)$$

where N is the power-law exponent, which takes positive, but not necessarily integer, values. In Fig. 1 the geometry and mechanical

characteristics of the FGM plate are represented. This power-law assumption reflects a simple rule of mixtures used to obtain the effective properties of the FGM.⁴ The material properties along the thickness of the plate, such as Young's modulus E , Poisson's ratio ν , and mass density ρ can be determined according to Eqs. (2–4), yielding

$$E(\zeta) = (E_1 - E_2)V_1 + E_2 = \sqrt{E_1 E_2} E_{\text{fgm}}(\zeta) \quad (5)$$

$$\nu(\zeta) = (\nu_1 - \nu_2)V_1 + \nu_2 = \sqrt{\nu_1 \nu_2} \nu_{\text{fgm}}(\zeta) \quad (6)$$

$$\rho(\zeta) = (\rho_1 - \rho_2)V_1 + \rho_2 = \sqrt{\rho_1 \rho_2} \rho_{\text{fgm}}(\zeta) \quad (7)$$

where $E_{\text{fgm}}(\zeta)$, $\nu_{\text{fgm}}(\zeta)$, and $\rho_{\text{fgm}}(\zeta)$ are given as follows:

$$E_{\text{fgm}}(\zeta) = \left(\sqrt{E_1/E_2} - \sqrt{E_2/E_1}\right)V_1 + \sqrt{E_2/E_1} \quad (8)$$

$$\nu_{\text{fgm}}(\zeta) = \left(\sqrt{\nu_1/\nu_2} - \sqrt{\nu_2/\nu_1}\right)V_1 + \sqrt{\nu_2/\nu_1} \quad (9)$$

$$\rho_{\text{fgm}}(\zeta) = \left(\sqrt{\rho_1/\rho_2} - \sqrt{\rho_2/\rho_1}\right)V_1 + \sqrt{\rho_2/\rho_1} \quad (10)$$

It is worth noting that subscripts 1 and 2 in the material properties (E , ν , and ρ) stand for the corresponding properties of the ceramic and metallic constituents. Moreover, mechanical properties, Eqs. (5–7), vary through the thickness of the FGM plate in accordance with a nonsymmetric power law, so that the reference plane is not a plane of symmetry for the plate.

In the present study, it is assumed that the damping is internal; this damping is postulated to be representable as an equivalent viscous damping with c_1 , c_2 denoting the associated damping coefficients to the ceramic and metallic constituents, respectively. In particular, the local effective damping c at a given point of the plate is assumed to vary according to the power-law distribution following Eq. (4):

$$c(\zeta) = (c_1 - c_2)V_1 + c_2 \quad (11)$$

The hypothesis of proportional damping is adopted hereinafter:

$$c_1/c_2 = \rho_1/\rho_2$$

This assumption appears not to be restrictive; it corresponds to one of the possible realizations of the proportional damping in the multi-degrees-of-freedom vibrational system. From this assumption, the following simplified power-law distribution for the damping coefficient is obtained:

$$c(\zeta) = \sqrt{c_1 c_2} \rho_{\text{fgm}}(\zeta) \quad (12)$$

in which $\rho_{\text{fgm}}(\zeta)$ is indicated in Eq. (10).

Method of Analysis

Let $u(\xi, \eta, \zeta, t)$, $v(\xi, \eta, \zeta, t)$, and $w(\xi, \eta, \zeta, t)$ denote the displacement components in the ξ , η , and ζ directions, respectively. The linear elastic strain energy for a three-dimensional solid is

$$\begin{aligned} \mathcal{U} = & \frac{abh}{16} \int_{-1}^1 \int_{-1}^1 \int_{-1}^1 \frac{E}{1+\nu} \left[\frac{1-\nu}{1-2\nu} (\varepsilon_{xx}^2 + \varepsilon_{yy}^2 + \varepsilon_{zz}^2) \right. \\ & + \frac{2\nu}{1-2\nu} (\varepsilon_{xx}\varepsilon_{yy} + \varepsilon_{xx}\varepsilon_{zz} + \varepsilon_{yy}\varepsilon_{zz}) \\ & \left. + \frac{1}{2} (\varepsilon_{xy}^2 + \varepsilon_{xz}^2 + \varepsilon_{yz}^2) \right] d\xi d\eta d\zeta \end{aligned} \quad (13)$$

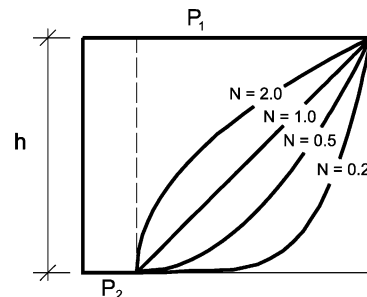
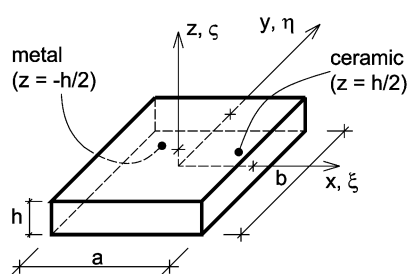


Fig. 1 Geometry and mechanical properties of the FGM plate.

where ε_{xx} , ε_{yy} , ε_{zz} , ε_{xz} , ε_{yz} , and ε_{xy} are the strain components. We suppose that the modulus of elasticity E and the Poisson's ratio ν are functions of the coordinate ζ , Eqs. (5) and (6), respectively.

The kinetic energy of the plate during the vibratory motion is

$$\mathcal{T} = \frac{abh}{16} \int_{-1}^1 \int_{-1}^1 \int_{-1}^1 \rho(\zeta) (\dot{u}^2 + \dot{v}^2 + \dot{w}^2) d\xi d\eta d\zeta \quad (14)$$

where the dot denotes differentiation with respect to time t and $\rho(\zeta)$ is given in Eq. (7).

A dissipation functional \mathcal{D} , introduced by Siu and Bert¹⁴ and Leissa^{15,16} and Leissa and Young¹⁷ (see also Elishakoff et al.¹⁸), is here extended for a three-dimensional solid:

$$\mathcal{D} = \frac{abh}{16} \int_{-1}^1 \int_{-1}^1 \int_{-1}^1 c(\zeta) (\dot{u}u + \dot{v}v + \dot{w}w) d\xi d\eta d\zeta \quad (15)$$

where $c(\zeta)$ is the viscous damping coefficient having the expression in Eq. (12). We consider a functionally graded plate subjected to a transverse harmonic force applied on the top surface,

$$q(\xi, \eta, t) = Q(\xi, \eta) \cos(\omega t) \quad (16)$$

where ω is the frequency of the exciting force. For sake of simplicity, in the right-hand side of Eq. (16) the expression $\cos(\omega t)$ is replaced by $e^{i\omega t}$, where $i = (-1)^{1/2}$. With this substitution, the modified governing equation yields a complex value of expression for the displacements; the real part of the final expression constitutes the sought solution. The work done by the exciting force is

$$\mathcal{W} = \frac{ab}{4} \int_{-1}^1 \int_{-1}^1 q(\xi, \eta, t) w(\xi, \eta, 1, t) d\xi d\eta \quad (17)$$

where $w(\xi, \eta, 1, t)$ is the transverse displacement evaluated at the upper surface, $\zeta = 1$.

To apply the Ritz method, we assume that the displacement components have the following expressions:

$$u(\xi, \eta, \zeta, t) = U(\xi, \eta, \zeta) e^{i\omega t}, \quad v(\xi, \eta, \zeta, t) = V(\xi, \eta, \zeta) e^{i\omega t} \\ w(\xi, \eta, \zeta, t) = W(\xi, \eta, \zeta) e^{i\omega t} \quad (18)$$

where $U(\xi, \eta, \zeta)$, $V(\xi, \eta, \zeta)$, and $W(\xi, \eta, \zeta)$ are expressed in terms of a series of Chebyshev polynomials in the following form:

$$U(\xi, \eta, \zeta) = F_u(\xi, \eta) \sum_i^I \sum_j^J \sum_k^K C_{ijk}^u P_i(\xi) P_j(\eta) P_k(\zeta) \\ V(\xi, \eta, \zeta) = F_v(\xi, \eta) \sum_l^L \sum_m^M \sum_n^N C_{lmn}^v P_l(\xi) P_m(\eta) P_n(\zeta) \\ W(\xi, \eta, \zeta) = F_w(\xi, \eta) \sum_p^P \sum_q^Q \sum_r^R C_{pqr}^w P_p(\xi) P_q(\eta) P_r(\zeta) \quad (19)$$

In Eq. (19) the generic function $P_s(\chi)$ is the one-dimensional s th Chebyshev polynomial; C_{ijk}^u , C_{lmn}^v , C_{pqr}^w are complex unknown coefficients to be determined; and F_u , F_v , F_w are appropriate boundary functions.

In general, in the representation of the displacement components Eq. (19), the number of terms in the ξ , η , and ζ directions can be different. In practice, the same number of terms, indicated with N_ξ , N_η , and N_ζ in the ξ , η , and ζ directions, are considered (i.e., $I = L = P = N_\xi$, $J = M = Q = N_\eta$, and $K = N = R = N_\zeta$).

The admissible function is selected to be the one-dimensional s th Chebyshev polynomial, which can be constructed according to the following recurrence relation¹⁹:

$$P_{s+1}(\chi) = 2\chi P_s(\chi) - P_{s-1}(\chi) \\ s = 1, 2, \dots, \quad \text{and} \quad \chi = \xi, \eta, \zeta$$

where $P_1(\chi) = 1$, $P_2(\chi) = \chi$, etc. It is known¹⁹ that Chebyshev polynomials constitute an orthogonal polynomial sequence with respect to the weight function $\varpi(\chi) = (1 - \chi^2)^{-1/2}$ on the interval $[-1, 1]$.

In numerical approximation, Chebyshev polynomials have shown high accuracy and better stability²⁰ compared with other polynomial series.

In this study a simply supported plate is considered. The boundary conditions are specified as follows:

$$\begin{aligned} v = 0, \quad w = 0, \quad \sigma_x = 0 \quad \text{at} \quad \xi = \pm 1 \\ u = 0, \quad w = 0, \quad \sigma_y = 0 \quad \text{at} \quad \eta = \pm 1 \end{aligned}$$

To satisfy the preceding edge conditions according to the Ritz formulation, F_u , F_v , and F_w in Eq. (19) can be expressed as a product of two one-dimensional functions in the ξ and η directions:

$$F_\delta(\xi, \eta) = f_\delta^1(\xi) f_\delta^2(\eta) \quad \text{with} \quad \delta = u, v, w$$

where $f_\delta^1(\xi)$ and $f_\delta^2(\eta)$ are given as follows:

$$\begin{aligned} f_u^1(\xi) = 1, \quad f_v^1(\xi) = 1 - \xi^2, \quad f_w^1(\xi) = 1 - \xi^2 \\ f_u^2(\eta) = 1 - \eta^2, \quad f_v^2(\eta) = 1, \quad f_w^2(\eta) = 1 - \eta^2 \end{aligned}$$

Solution Methodology

Leissa and Young¹⁷ generalized the functional $\mathcal{T}_{\max} - \mathcal{V}_{\max}$ used in free, undamped vibration analysis by minimizing the following functional

$$\Pi_{\max} = (\mathcal{T}_{\max} - \mathcal{D}_{\max}) - (\mathcal{V}_{\max} - \mathcal{W}_{\max}) \quad (20)$$

where the terms on the right-hand side of Eq. (20) are the maximum values of the functionals already given by Eqs. (13), (14), (15), and (17), obtained from Eqs. (18) and (19) setting $|e^{2i\omega t}| = 1$. Thus, the expressions of the functionals in Eq. (20) result in

$$\mathcal{T}_{\max} = \frac{abh}{16} \omega^2 \sqrt{\rho_1 \rho_2} \int_{-1}^1 \int_{-1}^1 \int_{-1}^1 \rho_{\text{fgm}}(\zeta) \\ \times (U^2 + V^2 + W^2) d\xi d\eta d\zeta \quad (21)$$

$$\mathcal{D}_{\max} = \frac{abh}{16} i\omega \sqrt{c_1 c_2} \int_{-1}^1 \int_{-1}^1 \int_{-1}^1 \rho_{\text{fgm}}(\zeta) \\ \times (U^2 + V^2 + W^2) d\xi d\eta d\zeta \quad (22)$$

$$\mathcal{V}_{\max} = \frac{bh}{4a} \sqrt{E_1 E_2} \int_{-1}^1 \int_{-1}^1 \int_{-1}^1 \frac{E_{\text{fgm}}(\zeta) [1 - \nu(\zeta)]}{[1 + \nu(\zeta)][1 - 2\nu(\zeta)]} \\ \times \left\{ \left(\frac{\partial U}{\partial \xi} \right)^2 + \frac{a^2}{b^2} \left(\frac{\partial V}{\partial \eta} \right)^2 + \frac{a^2}{h^2} \left(\frac{\partial W}{\partial \zeta} \right)^2 \right. \\ \left. + \frac{2\nu(\zeta)}{1 - \nu(\zeta)} \left[\frac{a}{b} \frac{\partial U}{\partial \xi} \frac{\partial V}{\partial \eta} + \frac{a}{h} \frac{\partial U}{\partial \xi} \frac{\partial W}{\partial \zeta} + \frac{a^2}{hb} \frac{\partial V}{\partial \eta} \frac{\partial W}{\partial \zeta} \right] \right. \\ \left. + \frac{1 - 2\nu(\zeta)}{2[1 - \nu(\zeta)]} \left[\frac{a^2}{b^2} \left(\frac{\partial U}{\partial \eta} \right)^2 + \frac{a^2}{h^2} \left(\frac{\partial U}{\partial \zeta} \right)^2 + \left(\frac{\partial V}{\partial \xi} \right)^2 \right. \right. \\ \left. \left. + \frac{a^2}{h^2} \left(\frac{\partial V}{\partial \zeta} \right)^2 + \left(\frac{\partial W}{\partial \xi} \right)^2 + \frac{a^2}{b^2} \left(\frac{\partial W}{\partial \eta} \right)^2 + \frac{2a}{b} \frac{\partial U}{\partial \eta} \frac{\partial V}{\partial \xi} \right. \right. \\ \left. \left. + \frac{2a}{h} \frac{\partial U}{\partial \zeta} \frac{\partial W}{\partial \xi} + \frac{2a^2}{hb} \frac{\partial V}{\partial \zeta} \frac{\partial W}{\partial \eta} \right] \right\} d\xi d\eta d\zeta \quad (23)$$

$$\mathcal{W}_{\max} = \frac{abh}{4} \int_{-1}^1 \int_{-1}^1 Q(\xi, \eta) W(\xi, \eta, 1) d\xi d\eta \quad (24)$$

The Ritz method requires Π_{\max} in Eq. (20) to attain minimum, so that

$$\frac{\partial \Pi_{\max}}{\partial C_{ijk}^u} = 0, \quad \frac{\partial \Pi_{\max}}{\partial C_{lmn}^v} = 0, \quad \frac{\partial \Pi_{\max}}{\partial C_{pqr}^w} = 0 \quad (25)$$

which lead to the following governing equation:

$$\mathbf{RC} = (a^2/2h)\mathbf{Q} \quad (26)$$

where

$$\mathbf{C} = \begin{bmatrix} \mathbf{C}^u \\ \mathbf{C}^v \\ \mathbf{C}^w \end{bmatrix}, \quad \mathbf{Q} = \begin{bmatrix} 0 \\ 0 \\ \mathbf{Q}^z \end{bmatrix} \quad (27)$$

$$\mathbf{R} = \sqrt{E_1 E_2} \mathbf{K} + \left(\frac{\sqrt{c_1 c_2}}{\sqrt{\rho_1 \rho_2}} i \omega - \omega^2 \right) a^2 \sqrt{\rho_1 \rho_2} \mathbf{M} \quad (28)$$

with

$$\mathbf{K} = \begin{bmatrix} \mathbf{K}_{uu} & \mathbf{K}_{uv} & \mathbf{K}_{uw} \\ \mathbf{K}_{uv}^T & \mathbf{K}_{vv} & \mathbf{K}_{vw} \\ \mathbf{K}_{uw}^T & \mathbf{K}_{vw}^T & \mathbf{K}_{ww} \end{bmatrix}, \quad \mathbf{M} = \begin{bmatrix} \mathbf{M}_{uu} & 0 & 0 \\ 0 & \mathbf{M}_{vv} & 0 \\ 0 & 0 & \mathbf{M}_{ww} \end{bmatrix} \quad (29)$$

In Eqs. (26–29), \mathbf{C} and \mathbf{Q} are column vectors of the displacement coefficients and of the load of dimensions $3N_\xi N_\eta N_\zeta \times 1$, respectively, while \mathbf{K} and \mathbf{M} are the stiffness matrix and the mass matrix of dimensions $3N_\xi N_\eta N_\zeta \times 3N_\xi N_\eta N_\zeta$, respectively. The explicit form of the elements in the stiffness submatrices \mathbf{K}_{ij} with $i, j = u, v, w$ in Eq. (29) is given by

$$\begin{aligned} \mathbf{K}_{uu} &= D_{uii}^{11} E_{ujuj}^{00} F_{kk}^{00} + (a/b)^2 D_{uii}^{00} E_{ujuj}^{11} T_{kk}^{00} \\ &\quad + (a/h)^2 D_{uii}^{00} E_{ujuj}^{00} T_{kk}^{11} \\ \mathbf{K}_{uv} &= (a/b) (D_{uivl}^{10} E_{ujvm}^{00} S_{kn}^{00} + D_{uivl}^{01} E_{ujvm}^{10} T_{kn}^{00}) \\ \mathbf{K}_{uw} &= (a/h) (D_{uiwp}^{10} E_{ujwq}^{00} S_{kr}^{01} + D_{uiwp}^{01} E_{ujwq}^{10} T_{kr}^{10}) \\ \mathbf{K}_{vv} &= (a/b)^2 D_{vvl}^{00} E_{vmvm}^{11} F_{nn}^{00} + (a/h)^2 D_{vvl}^{00} E_{vmvm}^{00} T_{nn}^{11} \\ &\quad + D_{vvl}^{11} E_{vmvm}^{00} T_{nn}^{00} \\ \mathbf{K}_{vw} &= (a^2/hb) (D_{vlp}^{00} E_{vmwq}^{10} S_{nr}^{01} + D_{vlp}^{00} E_{vmwq}^{01} T_{nr}^{10}) \\ \mathbf{K}_{ww} &= (a/h)^2 D_{wpw\bar{p}}^{00} E_{wqw\bar{q}}^{00} F_{r\bar{r}}^{11} + (a/b)^2 D_{wpw\bar{p}}^{00} E_{wqw\bar{q}}^{11} T_{r\bar{r}}^{00} \\ &\quad + D_{wpw\bar{p}}^{11} E_{wqw\bar{q}}^{00} T_{r\bar{r}}^{00} \end{aligned} \quad (30)$$

The elements in the mass submatrices \mathbf{M}_{ij} , with $i, j = u, v, w$ in Eq. (29) are given by

$$\begin{aligned} \mathbf{M}_{uu} &= \frac{1}{4} D_{uii}^{00} E_{ujuj}^{00} M_{kk}, \quad \mathbf{M}_{vv} = \frac{1}{4} D_{vvl}^{00} E_{vmvm}^{00} M_{nn} \\ \mathbf{M}_{ww} &= \frac{1}{4} D_{wpw\bar{p}}^{00} E_{wqw\bar{q}}^{00} M_{r\bar{r}} \end{aligned} \quad (31)$$

where

$$\begin{aligned} D_{\alpha\beta\theta}^{rs} &= \int_{-1}^1 \frac{d^r [f_\alpha^1(\xi) P_\sigma(\xi)]}{d\xi^r} \frac{d^s [f_\beta^1(\xi) P_\theta(\xi)]}{d\xi^s} d\xi \\ E_{\alpha\beta\theta}^{rs} &= \int_{-1}^1 \frac{d^r [f_\alpha^2(\eta) P_\sigma(\eta)]}{d\eta^r} \frac{d^s [f_\beta^2(\eta) P_\theta(\eta)]}{d\eta^s} d\eta \\ F_{\sigma\theta}^{rs} &= \int_{-1}^1 \frac{E_{\text{figm}}(\zeta) (1 - \nu(\zeta))}{[1 + \nu(\zeta)][1 - 2\nu(\zeta)]} \frac{d^r P_\sigma(\zeta)}{d\zeta^r} \frac{d^s P_\theta(\zeta)}{d\zeta^s} d\zeta \\ S_{\sigma\theta}^{rs} &= \int_{-1}^1 \frac{E_{\text{figm}}(\zeta) \nu(\zeta)}{[1 + \nu(\zeta)][1 - 2\nu(\zeta)]} \frac{d^r P_\sigma(\zeta)}{d\zeta^r} \frac{d^s P_\theta(\zeta)}{d\zeta^s} d\zeta \\ T_{\sigma\theta}^{rs} &= \int_{-1}^1 \frac{E_{\text{figm}}(\zeta)}{2[1 + \nu(\zeta)]} \frac{d^r P_\sigma(\zeta)}{d\zeta^r} \frac{d^s P_\theta(\zeta)}{d\zeta^s} d\zeta \\ M_{\sigma\theta} &= \int_{-1}^1 \rho_{\text{figm}}(\zeta) P_\sigma(\zeta) P_\theta(\zeta) d\zeta \end{aligned}$$

$$(\sigma = i, j, k, l, m, n, p, q, r; \theta = \bar{i}, \bar{j}, \bar{k}, \bar{l}, \bar{m}, \bar{n}, \bar{p}, \bar{q}, \bar{r})$$

where $r, s = 0, 1$; subscripts α, β indicate the corresponding displacement amplitude functions u, v , and w ; and $i, j, k, l, m, n, p, q, r$ are the summation indices from Eq. (19), as are $\bar{i}, \bar{j}, \bar{k}, \bar{l}, \bar{m}, \bar{n}, \bar{p}, \bar{q}, \bar{r}$, but they do not have necessarily the same value. In the preceding relations, the quantities $E_{\text{figm}}(\zeta)$, $\nu(\zeta)$, and $\rho_{\text{figm}}(\zeta)$ have the expressions in Eqs. (6), (8), and (10), respectively.

For convenience, the arbitrary amplitude load $Q(\xi, \eta)$ in Eq. (16) is represented in the general form of a double series:

$$Q(\xi, \eta) = \sum_\alpha \sum_\beta Q_{\alpha\beta} P_\alpha(\xi) P_\beta(\eta) \quad (32)$$

where $Q_{\alpha\beta}$ is the generic coefficient and $P_\alpha(\xi)$, $P_\beta(\eta)$ are Chebyshev polynomials. According to Eq. (32), the element \mathbf{Q}^z of the load vector \mathbf{Q} in Eq. (27) reads

$$\begin{aligned} \mathbf{Q}^z &= \sum_\alpha \sum_\beta Q_{\alpha\beta} \int_{-1}^1 P_\alpha(\xi) P_\beta(\eta) f_w^1(\xi) d\xi \\ &\quad \times \int_{-1}^1 P_\beta(\eta) P_q(\eta) f_w^2(\eta) d\eta P_r(1) \end{aligned} \quad (33)$$

In view of Eq. (26), to evaluate the response, the \mathbf{R} matrix in Eq. (28) needs to be determined numerically. From Eq. (26), a set of equations has to be solved for the real and imaginary parts of the vector of the complex displacement coefficients \mathbf{C} . Making use of the relation $x + iy = C e^{i\phi}$, where $C = \sqrt{x^2 + y^2}$ and $\tan \phi = y/x$, because the displacement amplitudes U, V , and W in Eq. (19) are complex, the displacement components of Eq. (18) are expressed as follows:

$$\begin{aligned} u(\xi, \eta, \zeta, t) &= U(\xi, \eta, \zeta) e^{i\omega t} = \bar{U}(\xi, \eta, \zeta) e^{i(\omega t - \phi_u)} \\ v(\xi, \eta, \zeta, t) &= V(\xi, \eta, \zeta) e^{i\omega t} = \bar{V}(\xi, \eta, \zeta) e^{i(\omega t - \phi_v)} \\ w(\xi, \eta, \zeta, t) &= W(\xi, \eta, \zeta) e^{i\omega t} = \bar{W}(\xi, \eta, \zeta) e^{i(\omega t - \phi_w)} \end{aligned} \quad (34)$$

where $\bar{U}, \bar{V}, \bar{W}, \phi_u, \phi_v$, and ϕ_w are the amplitude responses and the phase angles in the ξ, η , and ζ directions, respectively. The steady-state solution corresponding to the harmonic load in Eq. (16) is given by the real part of Eq. (34).

Results and Discussion

In the present analysis the natural frequencies are not needed to be known. However, as a byproduct of this study, they can be determined. The location of the maximum response uniquely determines the natural frequencies. On the other hand, it is instructive to solve the free undamped vibration problem from the present analysis by putting the load and the damping terms equal to zero in Eq. (26) and in Eq. (28), respectively. By means of these simplifications, the expression of the modified \mathbf{R} matrix becomes

$$\mathbf{R} = \sqrt{E_1 E_2} \mathbf{K} - \omega_n^2 a^2 \sqrt{\rho_1 \rho_2} \mathbf{M}$$

in which ω_n is the natural frequency.

In the following, a ceramic-metal functionally graded plate is considered. The two constituents of the plate consist of zirconia and aluminum. Young's modulus, Poisson's ratio, and mass density for the zirconia are²¹ $E_1 = 168$ GPa, $\nu_1 = 0.298$, and $\rho_1 = 5700$ kg/m³, and for the aluminum are²¹ $E_2 = 70$ GPa, $\nu_2 = 0.300$, and $\rho_2 = 2700$ kg/m³, respectively.

Free and Forced Vibrations for Homogeneous Plates

To perform verification of this study, one needs to compare the present solution to some benchmark problems. Several papers have been published on forced vibrations of classical plates. Siu and Bert¹⁴ presented a general forced-vibration analysis for laminated isotropic rectangular plates including material damping. Mindlin plate theory and the Rayleigh–Ritz method were used in order to obtain the solution. Forced damped vibrations of circular plates were investigated by Leissa¹⁶ by the Rayleigh–Ritz method; Leissa and Young¹⁷ studied forced vibrations of beams and rectangular plates.

Elishakoff et al.¹⁸ extended the approach by Leissa by means of Wilson trial functions for the forced-vibration problem of a cantilever beam.

In the paper by Laura and Duran,²² the response was calculated at various frequencies expressed as the ratio of the excitation frequency to the natural frequency; they also calculated static response corresponding to $\omega = 0$, as well as dynamic ones at $\omega/\omega_{n1} = 0.3, 0.5$, and 0.8 , where ω_{n1} is the first natural frequency. To be able to conduct a direct comparison with Laura and Duran,²² we first calculate natural frequencies for simply supported homogeneous aluminum square plates with thickness side ratios h/a equal to 0.1 and 0.2 . The natural frequencies are compared with those available in the literature and are listed in Table 1. A glance at the values in Table 1 (Refs. 13 and 23–29) reveals that our results are in excellent agreement with the exact natural frequencies given by Srinivas et al.²⁴

Now we turn to the computing of the forced-vibration response. For simplicity, we consider the amplitude load $Q(\xi, \eta)$ of Eq. (32) such that is uniform of intensity q_0 . To calculate any particular coefficient $Q_{\alpha\beta}$ of the series, both sides of Eq. (32) are multiplied by $P_{\alpha'}(\xi)P_{\beta'}(\eta)\varpi_{\xi}(\xi)\varpi_{\eta}(\eta)$, where $\varpi_{\xi}(\xi)$, $\varpi_{\eta}(\eta)$ are the weight functions, and integrated twice from -1 to 1 :

$$\begin{aligned} & \int_{-1}^1 \int_{-1}^1 Q(\xi, \eta) P_{\alpha'}(\xi) P_{\beta'}(\eta) \varpi_{\xi}(\xi) \varpi_{\eta}(\eta) d\xi d\eta \\ &= \sum_{\alpha} \sum_{\beta} Q_{\alpha\beta} \int_{-1}^1 P_{\alpha}(\xi) P_{\alpha'}(\xi) \varpi_{\xi}(\xi) d\xi \\ & \times \int_{-1}^1 P_{\beta}(\eta) P_{\beta'}(\eta) \varpi_{\eta}(\eta) d\eta \end{aligned} \quad (35)$$

Since

$$Q(\xi, \eta) = q_0 \quad (36)$$

Eq. (35) becomes

$$\begin{aligned} & q_0 \int_{-1}^1 P_{\alpha'}(\xi) \varpi_{\xi}(\xi) d\xi \int_{-1}^1 P_{\beta'}(\eta) \varpi_{\eta}(\eta) d\eta \\ &= \sum_{\alpha} \sum_{\beta} Q_{\alpha\beta} \int_{-1}^1 P_{\alpha}(\xi) P_{\alpha'}(\xi) \varpi_{\xi}(\xi) d\xi \\ & \times \int_{-1}^1 P_{\beta}(\eta) P_{\beta'}(\eta) \varpi_{\eta}(\eta) d\eta \end{aligned} \quad (37)$$

From the orthogonality property, the integrals in left-hand side of Eq. (37) are different from zero, and in particular equal to π ,

only when $\alpha' = \beta' = 1$, which means $P_{\alpha'}(\xi) = P_{\beta'}(\eta) = 1$. As a consequence, also α and β have to be equal unity, which means $P_{\alpha}(\xi) = P_{\beta}(\eta) = 1$. From these considerations, we obtain from Eq. (37) that the only load coefficient $Q_{\alpha\beta}$ different from zero is Q_{11} , and it is equal to q_0 . The following simplified expression of the component Q^z of the load vector Q in Eq. (27) is derived:

$$q_0 \int_{-1}^1 P_p(\xi) f_w^1(\xi) d\xi \int_{-1}^1 P_q(\eta) f_w^2(\eta) d\eta P_r(1)$$

An equivalent critical damping c_{c1} is expressed in terms of the first natural frequency ω_{n1} :

$$c_{c1} = 2\sqrt{\rho_1 \rho_2} \omega_{n1}$$

The ratio

$$\delta_1 = \sqrt{c_1 c_2} / c_{c1}$$

is introduced, so that the expression for $\sqrt{c_1 c_2} / \sqrt{\rho_1 \rho_2}$ appeared in Eq. (28) becomes

$$\sqrt{c_1 c_2} / \sqrt{\rho_1 \rho_2} = 2\delta_1 \omega_{n1}$$

Thus, the matrix R in Eq. (28) can be rewritten in terms of these new quantities:

$$R = \sqrt{E_1 E_2} K + \omega_{n1}^2 \gamma (2i\delta_1 - \gamma) \sqrt{\rho_1 \rho_2} a^2 M$$

where $\gamma = \omega / \omega_{n1}$. From Eq. (26), the vector of the displacement coefficients C can be found. Substituting the elements of C in Eq. (19), a complex value for the amplitude displacements is found. To obtain the response, the real part of it needs to be evaluated.

In Table 2, the nondimensional transverse displacement amplitude for a homogeneous square aluminum plate with thickness-side ratio $h/a = 0.01$ is compared with the results given by Laura and Duran.²² In this case the viscous damping is not considered; the static

Table 2 Comparison of the displacement amplitudes $W(0, 0, 0)$ $E_2 h^3 / [12(1 - \nu_2^2) a^4 q_0]$ for the dynamic case for a homogeneous square aluminum plate with thickness-side ratio $h/a = 0.01$

$\gamma = \omega / \omega_{n1}$	Laura and Duran ²²	Classical solution ²²	Present solution
0	0.004062	0.00406	0.004064
0.3	0.0045	0.004473	0.004475
0.5	0.0055	0.005448	0.00545
0.8	0.0115	0.011445	0.01146

Table 1 Comparison study of the first five frequency parameters $\bar{\omega}_n = \omega_n a^2 / h \sqrt{(\rho_2 / E_2)}$ for a homogeneous aluminum square plate with $9 \times 9 \times 6$ terms in the Ritz series

h/a	Method of solution	$\bar{\omega}_{n1}$	$\bar{\omega}_{n2}$	$\bar{\omega}_{n3}$	$\bar{\omega}_{n4}$	$\bar{\omega}_{n5}$
0.1	Classical theory, Leissa ²³	5.9734	14.9334	14.9334	23.8934	29.8668
	Classical theory, Bhat ²⁵	5.9733	14.9334	14.9334	23.8935	30.0508
	Mindlin theory, Liew et al. ²⁶	5.7673	13.7537	13.7537	21.0979	25.7004
	Three-dimensional solution, Liew et al. ²⁷	5.7768	13.8050	13.8050	19.4833	19.4833
	Three-dimensional solution, Liew et al. ²⁸	5.7768	13.8134	13.8134	19.4833	19.4833
	Three-dimensional solution, Malik and Bert ²⁹	5.7769	13.8050	13.8050	19.4834	19.4834
	Three-dimensional solution, Batra and Vel ¹³	5.7769	n.a. ^a	n.a. ^a	n.a. ^a	n.a. ^a
	Exact solution, Srinivas et al. ²⁴	5.7768	13.8050	13.8050	19.4859	19.4859
	Present three-dimensional solution	5.7769	13.8050	13.8050	19.4833	19.4833
	Classical theory, Leissa ²³	5.9734	14.9334	14.9334	23.8934	29.8668
0.2	Classical theory, Bhat ²⁵	5.9733	14.9334	14.9334	23.8935	30.0508
	Mindlin theory, Liew et al. ²⁶	5.2742	11.5214	11.5214	16.6445	19.6550
	Three-dimensional solution, Liew et al. ²⁷	5.3037	9.7416	9.7416	11.6454	11.6454
	Three-dimensional solution, Liew et al. ²⁸	5.3037	9.7416	9.7416	11.6477	11.6477
	Three-dimensional solution, Malik and Bert ²⁹	5.3036	9.7417	9.7417	11.6454	11.6454
	Exact solution, Srinivas et al. ²⁴	5.3036	9.7417	9.7417	n.a. ^a	n.a. ^a
	Present three-dimensional solution	5.3036	9.7417	9.7417	11.6454	11.6454

^an.a. = not available.

displacement ($\gamma = 0$) and the dynamic response close to the resonance condition ($\gamma = 0.3, 0.5$, and 0.8) are calculated. The results for the response at the center of the plate yielded nearly identical comparisons.

Forced Vibrations for FGM Plates

After the preceding comparison studies for free and forced vibrations in order to verify the present approach for homogeneous plates, now forced vibrations of FGM square plates are investigated.

In the following, a square plate with thickness-side ratio $h/a = 0.2$ and four different values of the exponent $N = 0.2, 0.5, 1$, and 2 is considered. The viscous damping is small $\delta_1 = 0.01$ (Ref. 17). The ratio

$$R_w = Re[\bar{W} e^{i(\omega t - \phi_w)}] / W_{st} = W^R / W_{st}$$

between the real part of the dynamic response amplitude W^R and the static displacement W_{st} in the ζ direction at the center of the plate is introduced. The results obtained for R_w calculated at different values of the frequency ratio γ are listed in Table 3. For comparison purposes, also the extreme cases of homogeneous plates made of aluminum and zirconia are considered.

As expected, the ratio R_w becomes larger as the frequency ratio γ approaches the unity. The value of R_w is not always in between

Table 3 R_w for a FGM square plate ($h/a = 0.2$) at different values of the frequency ratio

$\gamma = \omega/\omega_{n1}$	Zirconia	$N = 0.2$	$N = 0.5$	$N = 1$	$N = 2$	Aluminum
0	1	1	1	1	1	1
0.8	2.8415	2.8415	2.8416	2.8423	2.8444	2.8416
0.95	10.4146	10.4143	10.4148	10.4187	10.4298	10.4148
1	51.9287	51.9264	51.9293	51.9509	52.0127	51.9295
1.05	9.9676	9.9670	9.9676	9.9722	9.9855	9.9677

the two extreme values of the pure metal and pure ceramic plate. For example, at the resonance condition the FGM plate with $N = 2$ presents the greatest value of R_w . This can be because the homogeneous aluminum plate has the greatest values of both the static and dynamic displacements at the plate center, whereas their ratio R_w is actually larger than the FGM plate with $N = 2$.

In Fig. 2, results for the nondimensional deflection in the thickness direction of a functionally graded plate for different values of the exponent N are plotted. The nondimensional transverse deflection is represented in Figs. 2a–2d for the case of the static load ($\gamma = 0$) and for $\gamma = 0.8, 0.95$, and 1 , respectively. It can be seen that the response for the FGM plates presents intermediate values between the pure metal plate and the pure ceramic plate also in the resonance condition.

From these figures it can be pointed out that the gradients in material properties play an important role in determining the dynamic response of FGM plates, both in and outside the resonance condition.

The through-the-thickness variation of the nondimensional in-plane displacement $100h^2 E_2 U^R / (q_0 a^3)$, evaluated at $(\xi, \eta) = (1/2, 1/2)$, for FGM plates are represented for different values of γ and N in Figs. 3–6, where U^R is the real part of $\bar{U} e^{i(\omega t - \phi_u)}$ in Eq. (34). The nondimensional in-plane displacement of a pure aluminum square plate is also represented for comparison purposes.

In Fig. 3 the behavior of the nondimensional in-plane displacement for a functionally graded square plate with $N = 0.2$ is depicted. The displacement is evaluated for the static case ($\gamma = 0$), in the resonance condition ($\gamma = 1$), and close to the resonance condition ($\gamma = 0.95$). Similarly to the behavior of the transverse displacement, the in-plane displacement is minimum when $\gamma = 0$, and it becomes larger as the ratio γ approaches to unity.

In Figs. 4–6, the nondimensional in-plane displacement in the thickness direction for functionally graded plates with $N = 0.5, 1$, and 2 is represented, respectively.

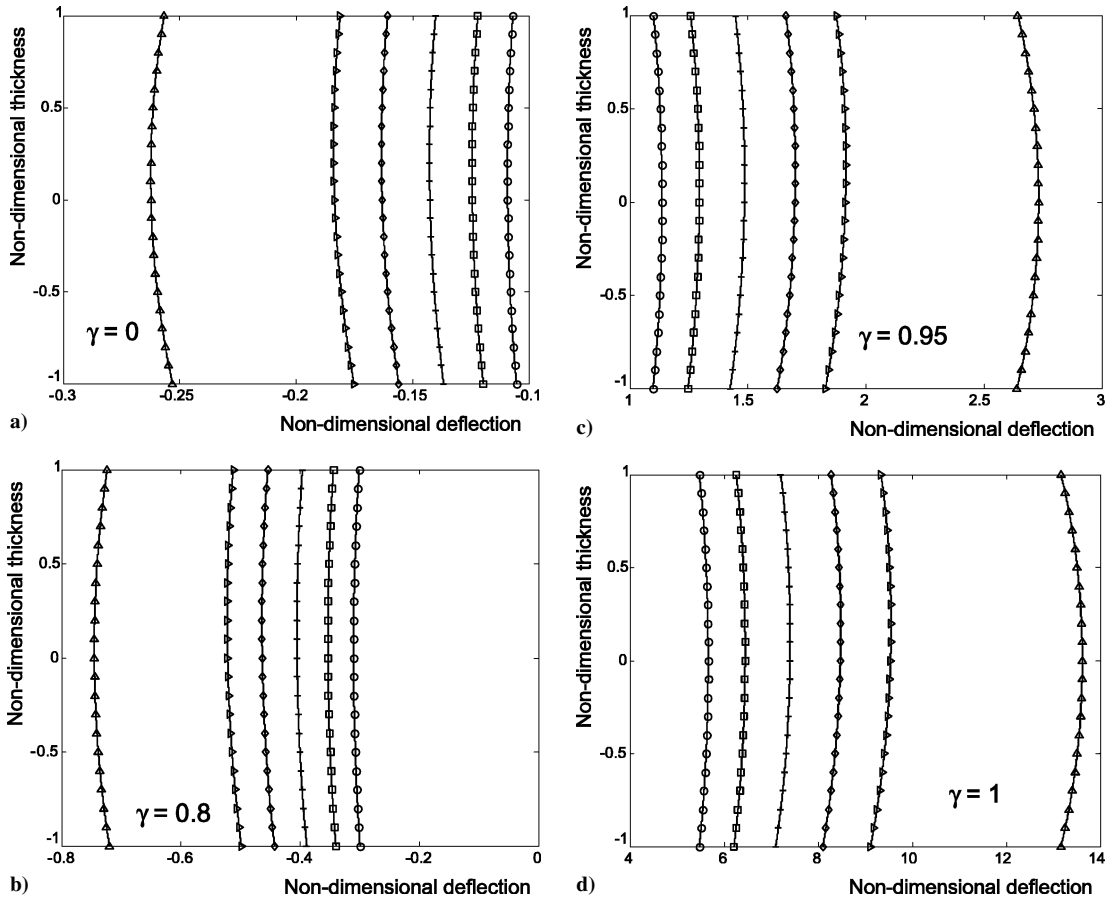


Fig. 2 Nondimensional deflection $100h^2 E_2 W^R / (q_0 a^3)$ vs nondimensional thickness ζ for FG and homogeneous plates (Δ , pure aluminum plate; \square , $N = 0.2$; $+$, $N = 0.5$; \diamond , $N = 1$; \triangleright , $N = 2$; and \circ , pure ceramic plate): a) $\gamma = 0$, static case; b) $\gamma = 0.8$; c) $\gamma = 0.95$; and d) $\gamma = 1$, resonance condition.

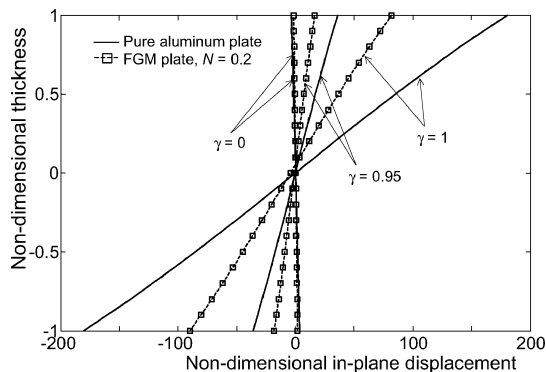


Fig. 3 Through-the-thickness variation of the nondimensional in-plane displacement for a pure aluminum plate and a FG plate with $N = 0.2$ for different values of γ .

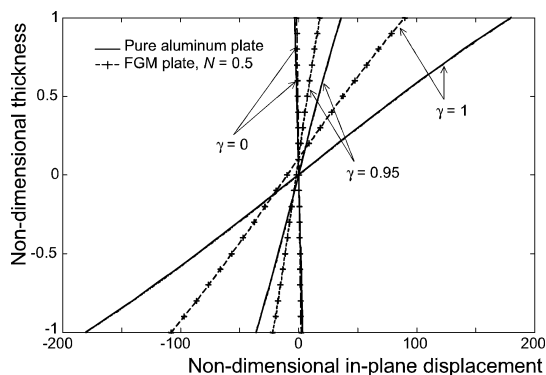


Fig. 4 Through-the-thickness variation of the nondimensional in-plane displacement for a pure aluminum plate and a FG plate with $N = 0.5$ for different values of γ .

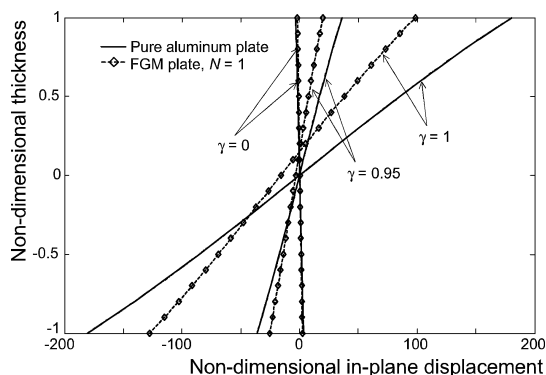


Fig. 5 Through-the-thickness variation of the nondimensional in-plane displacement for a pure aluminum plate and a FG plate with $N = 1$ for different values of γ .

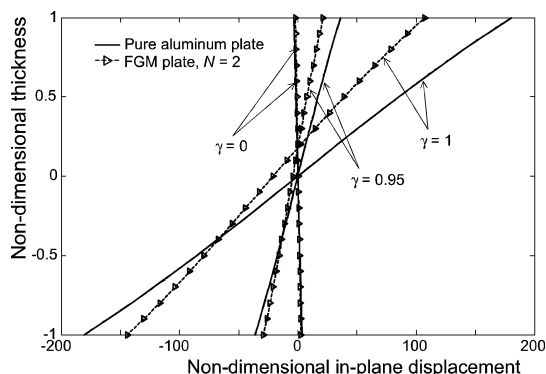


Fig. 6 Through-the-thickness variation of the nondimensional in-plane displacement for a pure aluminum plate and a FG plate with $N = 2$ for different values of γ .

It can be seen that the differences between the in-plane displacement for the functionally graded plates and the homogeneous one at the bottom and upper surfaces ($\zeta = \pm 1$) become smaller with the increasing of the value of the exponent N . In particular, the point where the homogeneous plate and the functionally graded plate share the same in-plane displacement is moving towards the bottom surface of the plate. This is expected because the more N becomes large the more the ceramic content is low and the functionally graded plate approaches the case of the fully metallic plate.

Conclusions

A three-dimensional elasticity solution to the problem of forced, damped vibrations of simply supported rectangular plates made of a two-phase functionally graded material has been presented. The material properties of the constituents, such as modulus of elasticity, Poisson's ratio, mass density and damping coefficient are assumed to vary in the thickness direction in accordance with a power law. The solution is obtained by a generalized Rayleigh–Ritz method, which incorporates both the material damping and the external force. From the present method, natural frequencies and static solutions can be determined by setting the load and dissipation terms, and the forcing frequency, equal to zero in the expression of the generalized energy functional, respectively.

The results obtained for forced, damped vibration analysis of the FGM plates are supported by appropriate comparisons with results available in the literature for the case of simply supported homogeneous plates. No comparisons with analytical results for forced damped vibrations of FGM plates could be made, because apparently they have not been available previously. Parametric studies have been performed for varying the power-law exponent and thickness-side ratio. From the numerical results it can be seen that when the excitation frequency is close or equal to the fundamental natural frequency the gradients in material properties play an important role in determining the dynamic response of the FGM plates. This means that the property gradients can be appropriately tailored in order to control the magnitude of the dynamic response at the resonance condition. It should be remarked that the concepts outlined in this study are not confined to simply supported plates, but they can be extended to other boundary conditions.

Acknowledgments

Isaac Elishakoff thanks the J. M. Rubin Foundation for partial financial support. This research was conducted when Cristina Gentilini served as a visiting scholar at the Mechanical Engineering Department at Florida Atlantic University (FAU). The financial support of the Italian Ministry for Education, University and Research and University of Bologna ("Progetto Marco Polo") as well as kind and warm hospitality by the FAU faculty and staff are gratefully acknowledged.

References

- Koizumi, M., "FGM Activities in Japan," *Composites Part B: Engineering*, Vol. 28, No. 1–2, 1997, pp. 1–4.
- Suresh, S., and Mortensen, A., *Fundamentals of Functionally Graded Materials*, Inst. of Materials, London, 1998.
- Fukui, Y., "Fundamental Investigation of Functionally Gradient Material Manufacturing System Using Centrifugal Force," *JSME International Journal Series III*, Vol. 34, No. 1, 1991, pp. 144–148.
- Praveen, G. N., and Reddy, J. N., "Nonlinear Transient Thermoelastic Analysis of Functionally Graded Ceramic-Metal Plates," *International Journal of Solids and Structures*, Vol. 35, No. 33, 1998, pp. 4457–4476.
- Cheng, Z.-Q., and Batra, R. C., "Exact Correspondence Between Eigenvalues of Membranes and Functionally Graded Simply Supported Polygonal Plates," *Journal of Sound and Vibration*, Vol. 229, No. 4, 2000, pp. 879–895.
- Reddy, J. N., "Analysis of Functionally Graded Plates," *International Journal for Numerical Method in Engineering*, Vol. 47, No. 1–3, 2000, pp. 663–684.
- Ng, T. Y., Lam, K. Y., and Liew, K. M., "Effects of FGM Materials on the Parametric Resonance of Plate Structures," *Computer Methods in Applied Mechanics and Engineering*, Vol. 190, No. 8–10, 2000, pp. 953–962.
- Yang, J., and Shen, H.-S., "Vibration Characteristics and Transient Response of Shear-Deformable Functionally Graded Plates in Thermal

Environments," *Journal of Sound and Vibration*, Vol. 255, No. 3, 2002, pp. 579–602.

⁹Pradhan, S. C., Loy, C. T., Lam, K. Y., and Reddy, J. N., "Vibration Characteristics of Functionally Graded Cylindrical Shells Under Various Boundary Conditions," *Applied Acoustics*, Vol. 61, No. 1, 2000, pp. 111–129.

¹⁰Yang, J., and Shen, H. -S., "Free Vibration and Parametric Resonance of Shear Deformable Functionally Graded Cylindrical Panels," *Journal of Sound and Vibration*, Vol. 261, No. 5, 2003, pp. 871–893.

¹¹Yang, J., Kitipornchai, S., and Liew, K. M., "Large Amplitude Vibration of Thermo-Electro-Mechanically Stressed FGM Laminated Plates," *Computer Methods in Applied Mechanics and Engineering*, Vol. 192, No. 35–36, 2003, pp. 3861–3885.

¹²Kitipornchai, S., Yang, J., and Liew, K. M., "Semi-Analytical Solution for Non-Linear Vibration of Laminated FGM Plates with Geometric Imperfections," *International Journal of Solids and Structures*, Vol. 41, No. 9–10, 2004, pp. 2235–2257.

¹³Vel, S. S., and Batra, R. C., "Three-Dimensional Exact Solution for the Vibration of Functionally Graded Rectangular Plates," *Journal of Sound and Vibration*, Vol. 272, No. 3–5, 2004, pp. 703–730.

¹⁴Siu, C. C., and Bert, C. W., "Sinusoidal Response of Composite-Material Plates with Material Damping," *Journal of Engineering for Industry*, Vol. 96, May 1974, pp. 603–610.

¹⁵Leissa, A. W., "A Direct Method for Analyzing the Forced Vibrations of Continuous Systems Having Damping," *Journal of Sound and Vibration*, Vol. 56, No. 3, 1978, pp. 313–324.

¹⁶Leissa, A. W., "The Analysis of Forced Vibrations of Plates Having Damping," *Proceedings of the Ninth Southeastern Conference on Theoretical and Applied Mechanics*, Vol. 9, Plenum Press, New York, 1978, pp. 183–193.

¹⁷Leissa, A. W., and Young, T. H., "Extensions of the Ritz–Galerkin Method for the Forced, Damped Vibrations of Structural Elements," *Proceedings of the Vibration Damping Workshop*, Wright–Patterson AFB, OH, 1984, pp. EE1–EE22.

¹⁸Elishakoff, I., Hettema, C. D., and Wilson, E. L., "Direct Superposition of Wilson Trial Functions by Computerized Symbolic Algebra," *Acta Mechanica*, Vol. 74, 1988, pp. 69–79.

¹⁹Snyder, M. A., *Chebyshev Methods in Numerical Approximation*, Prentice–Hall, Englewood Cliffs, NJ, 1966.

²⁰Zhou, D., Cheung, Y. K., Au, F. T. K., and Lo, S. H., "Three Dimensional Vibration Analysis of Thick Rectangular Plates Using Chebyshev Polynomial and Ritz Method," *International Journal of Solids and Structures*, Vol. 39, No. 26, 2002, pp. 6339–6353.

²¹Touloukian, Y. S., *Thermophysical Properties of High Temperature Solid Materials*, Macmillan, New York, 1967.

²²Laura, P. A. A., and Duran, R., "A Note on Forced Vibrations of a Clamped Rectangular Plate," *Journal of Sound and Vibration*, Vol. 42, No. 1, 1975, pp. 129–135.

²³Leissa, A. W., "The Free Vibration of Rectangular Plates," *Journal of Sound and Vibration*, Vol. 31, No. 3, 1973, pp. 257–293.

²⁴Srinivas, S., Joga Rao, C. V., and Rao, A. K., "An Exact Analysis for Vibration of Simple-Supported Homogeneous and Laminated Thick Rectangular Plates," *Journal of Sound and Vibration*, Vol. 12, No. 2, 1970, pp. 187–199.

²⁵Bhat, R. B., "Natural Frequencies of Rectangular Plates Using Characteristic Orthogonal Polynomials in Rayleigh–Ritz Method," *Journal of Sound and Vibration*, Vol. 102, No. 4, 1985, pp. 493–499.

²⁶Liew, K. M., Hung, K. C., and Lim, M. K., "Vibration of Mindlin Plates Using Boundary Characteristic Orthogonal Polynomials," *Journal of Sound and Vibration*, Vol. 182, No. 1, 1995, pp. 77–90.

²⁷Liew, K. M., Hung, K. C., and Lim, M. K., "Three-Dimensional Vibration of Rectangular Plates: Effects of Thickness and Edge Constraints," *Journal of Sound and Vibration*, Vol. 182, No. 5, 1995, pp. 709–727.

²⁸Liew, K. M., and Teo, T. M., "Three-Dimensional Vibration Analysis of Rectangular Plates Based on Differential Quadrature Method," *Journal of Sound and Vibration*, Vol. 220, No. 4, 1999, pp. 577–599.

²⁹Malik, M., and Bert, C. W., "Three-Dimensional Elasticity Solutions for Free Vibrations of Rectangular Plates by the Differential Quadrature Method," *International Journal of Solids and Structures*, Vol. 35, No. 3–4, 1998, pp. 299–318.

A. Messac
Associate Editor